

GRAVITATIONAL WAVES FROM MERGING INTERMEDIATE-MASS BLACK HOLES : II EVENT RATES AT GROUND-BASED DETECTORS

HISA-AKI SHINKAI¹

Dept. of Information Science and Technology, Osaka Institute of Technology, Kitayama 1-79-1, Hirakata City, Osaka 573-0196, Japan

NOBUYUKI KANDA²

Dept. of Physics, Osaka City University, Sugimoto 3-3-138, Sumiyoshi, Osaka City, Osaka 558-8585, Japan

TOSHIKAZU EBISUZAKI³

Computational Astrophysics Laboratory, Institute of Physical and Chemical Research (RIKEN), Hirosawa 2-1, Wako City, Saitama 351-0198, Japan

¹hisaaki.shinkai@oit.ac.jp

²kanda@sci.osaka-cu.ac.jp

³ebisu@riken.jp

ABSTRACT

Based on a dynamical formation model of a super-massive black-hole (SMBH), we estimate expected observational profile of gravitational wave at ground-based detectors, such as KAGRA or advanced LIGO/VIRGO. Focusing that the second generation of detectors have enough sensitivity from 10 Hz and up (especially with KAGRA due to its location at less seismic noise), we are able to detect the ring-down gravitational wave of a BH of the mass $M < 2 \times 10^3 M_\odot$. This enables us to check the sequence of BH mergers to SMBH via intermediate-mass black-holes (IMBHs). We estimate the number density of galaxies from halo formation model, and estimate the number of BH mergers from giant molecular cloud model assuming hierarchical growth of merged cores. At the designed KAGRA (and/or advanced LIGO/VIRGO), we find that the BH mergers of its total mass $M \sim 60 M_\odot$ is at the peak of the expected mass distribution. With its signal-to-noise ratio $\rho = 10(30)$, we estimate the event rate $R \sim 200(20)$ per year in the most optimistic case, and we also find that BH mergers of the range $M < 150 M_\odot$ are $R > 1$ per year for $\rho = 10$. Thus if we observe a BH with more than $100 M_\odot$ in future gravitational wave observations, our model naturally explains its source.

Keywords: (Galaxy:) globular clusters: general — stars: black holes — (galaxies:) quasars: super-massive black holes — gravitational waves

1. INTRODUCTION

1.1. Era of gravitational wave astronomy

The direct detections of gravitational waves were announced by the advanced LIGO group in 2016 (Abbott et al. 2016a,b), and we are at the opening era of “gravitational wave astronomy”. LIGO group reported two events (GW150914, GW151226) and one transient event (LVT151012), all of three are regarded as the events of coalescence of binary black holes (BBHs).

The first event (GW150914) was the merger of BHs of the masses $36.2_{-3.8}^{+5.2} M_\odot$ and $29.1_{-4.4}^{+3.7} M_\odot$, which turned into a single BH of $62.3_{-3.1}^{+3.7} M_\odot$ with spin $a = 0.68_{-0.06}^{+0.05}$, which shows the energy radiation rate is 4.6% of the to-

tal mass. The event occurred at redshift $z = 0.09_{-0.04}^{+0.03}$, and detected with signal-to-noise ratio $\rho = 23.7$. The second event (GW151226) was the merger of BHs with $14.2_{-3.7}^{+8.3} M_\odot$ and $7.5_{-2.3}^{+2.3} M_\odot$, which turned into a single BH of $20.8_{-1.7}^{+6.1} M_\odot$ with spin $a = 0.74_{-0.06}^{+0.06}$, which shows the energy radiation rate is 4.1% of the total mass. The event occurred at redshift $z = 0.09_{-0.04}^{+0.03}$, and detected with $\rho = 13.0$ (These numbers were taken from Abbott et al. (2016c)).

These announcements were valuable not only on the point of the direct detections of the gravitational wave, but also the first results of confirming the existence of BH, the existence of BH of this mass range, and the

existence of BBHs. Especially, the existence of $\sim 30M_{\odot}$ BHs was surprising to the community, since there were no such observational evidences ever.

1.2. Possible sources of $30 M_{\odot}$ BHs

Traditional scenario for forming BBHs are common envelope evolution of primordial binary massive stars (Belczynski *et al.* 2007), and dynamical formation in dense star clusters (Portegies Zwart & McMillan 2000).

Several groups reported possible scenarios for making $30 M_{\odot}$ BHs. Kinugawa *et al.* (2014, 2016) proposed to use population III stars to form BBHs. Existence of population III stars is yet to be confirmed, but they show a typical BH mass of this model is at $\sim 30M_{\odot}$ (chirp mass $\sim 60M_{\odot}$), and the event rate would be 500 yr^{-1} (50 yr^{-1} for $\rho \geq 20$) (Nakano *et al.* 2015).

Recently, Fujii *et al.* (2016) estimate BH mergers combining their N-body simulations, modeling of globular clusters, and cosmic star-cluster formation history, and find that BH mass distribution has a peak at $10 M_{\odot}$ and $50 M_{\odot}$, and event rate for designed LIGO is at most 85 yr^{-1} .

In this article, based on a forming scenario of a supermassive black-hole (SMBH), we extend the previous model to a sequence of intermediate-mass black-hole (IMBHs), and estimate their observational detectability at ground-based gravitational wave detectors.

1.3. SMBH runaway path

Formation process of a SMBH is one of the unsolved problem in galaxy evolution history. Many possible routes were suggested by Rees (1978) long ago, but we still do not know the actual route in nature.

One possible scenario is by accumulations of BHs, which is supported by the discovery of IMBH (10^2 – $10^3 M_{\odot}$) in a starburst galaxy M82 (Matsumoto *et al.* 2001; Matsushita *et al.* 2000).

This runaway path was first proposed by Ebisuzaki *et al.* (2001). The scenario consists of three steps: (1) formation of IMBHs by runaway mergers of massive stars in dense star clusters (Portegies Zwart *et al.* 2004), (2) accumulations of IMBHs at the center region of a galaxy due to sinkages of clusters by dynamical friction, and (3) mergers of IMBHs by multi-body interactions and gravitational radiation. Successive mergers of IMBHs likely to form a SMBH with a mass of heavier than $> 10^6 M_{\odot}$. Ebisuzaki *et al.* (2001) predicted the IMBH-IMBH or IMBH-SMBH merging events can be observed on the order of one per month or even one per week.

Numerical simulations support the above first step (Marchant & Shapiro 1980; Portegies Zwart *et al.* 1999; Portegies Zwart & McMillan 2002; Portegies Zwart *et al.* 2004; Holger & Makino 2003),

and the second step is also confirmed in a realistic mass-loss model (Matsubayashi *et al.* 2007), while the third step is not yet investigated in detail. The discovery of a SMBH binary system (Sudou *et al.* 2003) together with a simulation of an eccentric evolution of SMBH binaries (Iwasawa *et al.* 2010) support this formation scenario through merging of IMBHs.

1.4. IMBH and gravitational waves

In Matsubayashi *et al.* (2004) (Paper I, hereafter), we pointed out that gravitational-wave from IMBHs can be a trigger to prove this process. If the space-based laser interferometers are in action, then their observation ranges (10^{-4} – 10 Hz) are quite reasonable for IMBH mergers. By accumulating data of merger events, we can distinguish the IMBH merger scenario such as they merge hierarchically or monopolistically.

Later, Fregeau *et al.* (2006) discussed the event rates of IMBH-IMBH binary observations at advanced LIGO and VIRGO, and concluded that we can expect ~ 10 mergers a year. This work was followed by Gair *et al.* (2011) including the Einstein Telescope project. Amaro-Seoane & Santamaria (2010) also concern the IMBH-IMBH system including pre-merger phase.

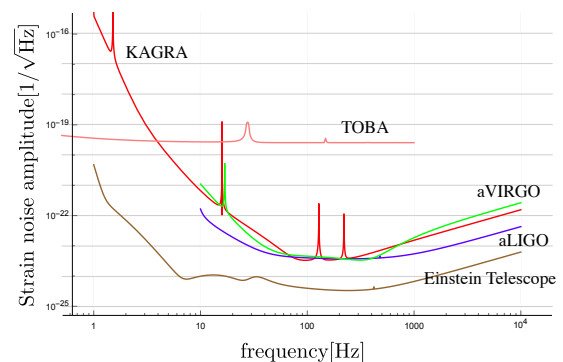


Figure 1. Designed strain noise amplitude of the advanced detectors (advanced LIGO, advanced VIRGO, and KAGRA), and planned Einstein Telescope. We also plotted that of torsion-balance antenna (TOBA).

Focusing that the second generation of GW interferometers have enough sensitivity at 10 Hz and above (see Fig.1), we are able to detect the ring-down gravitational wave of a BH of the mass $M < 2 \times 10^3 M_{\odot}$.

In this article, we therefore discuss how much we can observe BH mergers by finding their ring-down part using designed ground-based detectors. We roughly assume the mass distribution of BHs, $N(M)$, in a galaxy or globular cluster, which would be related to the merging history of BHs, and estimate the event rate using the designed strain noise of KAGRA, which is at the equivalent level with aLIGO/aVIRGO.

In addition, recent approaches to gravitational wave detection using a torsion-bar antenna (TOBA; (Ando *et al.* 2010; Ishidoshiro *et al.* 2011)) also quite attractive for this purpose since it covers the low frequency range (0.1 Hz \sim 10 Hz). However, the current strain noise amplitude of TOBA is larger compare to those of interferometers (see Fig.1), and we do not discuss the case of TOBA in this article.

The organization of the paper is as follows. In §2, we present the basic equations of gravitational radiation from IMBH binaries. In §3, we estimate the event rate of IMBH mergers under the simplest assumptions on galaxy distribution and formation process of SMBH. Summary and discussion are presented in §4. Throughout the paper, we use c and G for the light speed and gravitational constant, respectively.

2. BLACK HOLE MERGER MODEL

2.1. Ring-down frequency from BH

Gravitational waveform of binary-star merger which ends up with a single BH has typical three phases; inspiral phase, merging phase, and ring-down phase. The waveform in the inspiral phase is called as a “chirp signal” from its feature of increasing frequency and amplitude. For the case of GW150914, the frequency was first caught at 35 Hz, then it increased to 150 Hz, where the amplitude reached the maximum which indicates the merger of the binary. The final “ring-down” signal was supposed to be around 300 Hz.

As we mentioned in Paper I, for massive BH binaries with masses greater than $10^3 M_\odot$, the inspiral frequencies are less than 1 Hz. The wavelength of this frequency range is apparently more than the size of the Earth, so that its detection requires interferometers in space. On the other hand, the ring-down frequency is simply estimated by the quasi-normal frequency of BH, $f_R + if_I$, which is determined from the mass and spin of the final BH, and is estimated higher frequency than its inspiral phase. The quasi-normal modes are derived as eigenvalues of the wave equations on the perturbed geometry (see e.g. Leaver (1985)). For a BH with mass M_T and spin a , fitting functions are also known (Echeverria (1989); Berti *et al.* (2006)) in the form

$$f_R = f_1 + f_2(1 - a)^{f_3} \quad (1)$$

$$Q \equiv \frac{f_R}{2f_I} = q_1 + q_2(1 - a)^{q_3} \quad (2)$$

where Q is called the quality factor, and f_i, q_i are fitting coefficients. For the most fundamental mode, which is of the spherical harmonic index $\ell = 2, m = 2$, the fitting parameters are $f_1 = 1.5251, f_2 = -1.1568, f_3 = 0.1292, q_1 = 0.7000, q_2 = 1.4187$, and $q_3 = -0.4990$ (Berti *et al.* (2006)). Recovering the units, we can write

the frequency as

$$f_{\text{qnm}} = \frac{c^3}{2\pi G M_T} f_R \sim 3.2 \left(\frac{10 M_\odot}{M_T} \right) f_R [\text{kHz}]. \quad (3)$$

We plot f_{qnm} in Fig.2.

Supposing that advanced GW interferometers can detect f_{qnm} above 10 Hz, then BHs less than $1200 M_\odot$ are within the target if BHs are non-rotating ($a = 0$), while BHs less than $2500 M_\odot$ are in the detectable range for highly rotating cases ($a = 0.98$).

With this simple estimation, we hereafter consider mergers of BHs with those total mass is less than $2000 M_\odot$.

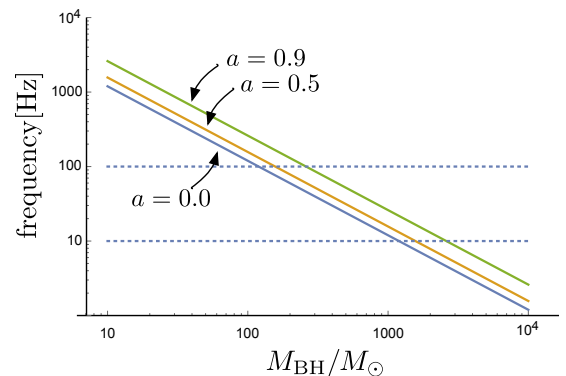


Figure 2. The quasi normal frequency f_{qnm} as a function of the mass of BH M_T . If we restrict the observable range is above 10 Hz for the advanced ground-based interferometers, then the BHs which mass are less than $2000 M_\odot$ are within the target.

2.2. Numbers of Galaxies in the Universe

In order to model the typical mass of galaxies and its distribution, We apply halo mass function discussed by Vale & Ostriker (2006). in which they discuss an empirically based, non-parametric model for galaxy luminosities with halo/subhalo masses. They apply Sheth-Tormen mass function (Sheth & Tormen 1999) for halo number density,

$$n_H(M)dM = 0.322 \left(1 + \frac{1}{\nu^{0.6}} \right) \sqrt{\frac{2}{\pi}} \frac{d\nu}{dM} \exp \left(-\frac{\nu^2}{2} \right) dM \quad (4)$$

where $\nu = \sqrt{a} \delta_c (1 + z) \sigma(M)$ with $a = 0.707$, the linear threshold for spherical collapse $\delta_c = 1.686$, and $\sigma(M)$ is the variance on the mass scale M . This mass function is roughly $\sim M^{-1.95}$ at low mass.

Vale & Ostriker (2006) also derive an average number of galaxies (subhalos) predicted for a parent halo of mass, which is roughly given by $N_{\text{subhalo}} \sim M^{0.9}$ (Fig.12 in their paper). If we regard this relation as

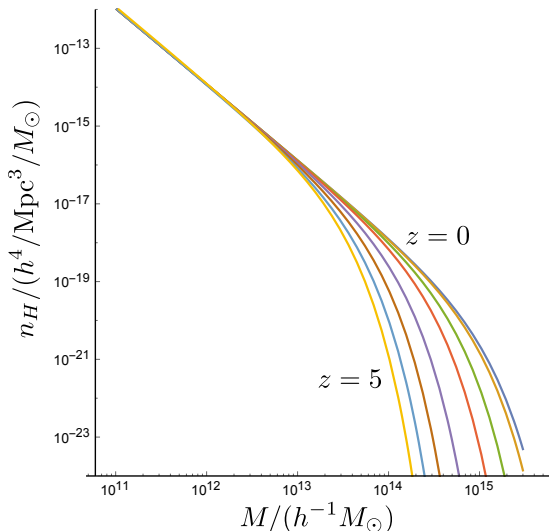


Figure 3. Global mass functions for halo (halo and subhalo), $n_H(M)$, for $z = 0, 0.1, 0.5, 2, 4, 5$ [eq.(4)]. $n_H(M)$ in units of $h^4/\text{Mpc}^3/M_\odot$. M in units of $h^{-1}M_\odot$, $h = 0.7$.

a seed of galaxies, then it indicates a typical galaxy has mass $10^{11} - 10^{12}M_\odot$.

Integrating (4) by the volume as a function of redshift z , we can derive the number density of halo. In this process, we use the standard cosmology model with current parameters, i.e. we use flat Friedmann model with Hubble constant $H_0=72$ km/s/Mpc, matter and dark matter density $\Omega_{m0} = 0.27$, and dark energy (cosmological constant) $\Omega_{d0} = 0.73$. The luminosity distance $d_L(z)$ is given by

$$d_L(z) = (1+z) \int_0^z \frac{c dz}{H(z)} \quad (5)$$

where

$$H(z) = H_0 \sqrt{(1+z)^3 \Omega_{m0} + \Omega_{d0}}. \quad (6)$$

The volume of the Universe is $V(d) = 4\pi d^3/3$.

Combining these two functions (average number of galaxies and the number density of halo), we get the number density of galaxy $n_{\text{galaxy}}(M, z)$, which we show in Fig.4. If we integrate it by M and z as

$$N_{\text{galaxy}}(z) = \int_0^z dz \int_{M_1}^{M_2} n_{\text{galaxy}}(M, z) dM, \quad (7)$$

then we get the number of galaxies. We set $M_1 = 10^9 M_\odot$ and $M_2 = 10^{13} M_\odot$.

From the recent ultra-violet luminosity density of star forming galaxies, star formation rate density $\rho_{\text{SFR}}(z)$ is fit as

$$\rho_{\text{SFRp}}(z) = \frac{0.009 + 0.27(z/3.7)^{2.5}}{1 + (z/3.7)^{7.4}} + 10^{-3} \quad (8)$$

$$\rho_{\text{SFRr}}(z) = \frac{0.009 + 0.27(z/3.4)^{2.5}}{1 + (z/3.4)^{8.3}} + 10^{-4} \quad (9)$$

for metal poor stars and metal rich stars, respectively

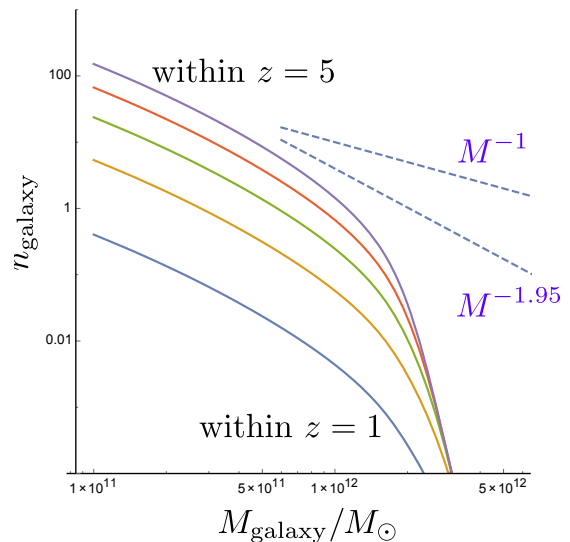


Figure 4. Number density of galaxy, $n_{\text{galaxy}}(M)$.

(Robertson *et al.* 2010). If we sum these two (normalized ρ_{SFRp} and normalized ρ_{SFRr}) evenly, the peak location is at $z = 3.26$. We then obtain

$$N_{\text{galaxy}}(z) = \int_0^z \rho_{\text{SFR}}(z) dz \int_{M_1}^{M_2} n_{\text{galaxy}}(M, z) dM. \quad (10)$$

The typical numbers of our model are shown in Table.1. These numbers are slightly larger than the latest observation by Conselice *et al.* (2016), but our model produces the same order and its evolution history for N_{galaxy} with them.

Table 1. Typical numbers of our galaxy model: the number of galaxy $N_{\text{galaxy}}(z)$, eq. (10), and the number density of galaxy n_{galaxy} .

z	$N_{\text{galaxy}}(z)$	n_{galaxy}
1	1.18×10^9	$1.0 \times 10^{-3}/\text{Mpc}^3$ for $z < 1$
2	9.45×10^{10}	$6.5 \times 10^{-3}/\text{Mpc}^3$ for $1 < z < 2$
3	5.23×10^{12}	$2.4 \times 10^{-2}/\text{Mpc}^3$ for $2 < z < 3$

2.3. Numbers of BHs in a galaxy

We next estimate a number of BH candidates in a galaxy. Recently, Inutsuka *et al.* (2015) developed a scenario of galactic-scale star formation from a giant molecular cloud. Their model includes both growth of molecular clouds and destruction of magnetized molecular clouds by radiation. Simulations and steady state analysis show that mass density function of molecular clouds, $n_{\text{cl}}(M_g)$, converges at the Schechter-like function,

$$n_{\text{cl}}(M_{\text{cl}}) \sim M_{\text{cl}}^{-1.7} \exp\left(-\frac{M_{\text{cl}}}{M_{\text{cut}}}\right) \quad (11)$$

where the cut-off mass $M_{\text{cut}} = 10^6 M_\odot$.

On the other hand, many N-body simulations report that there is a simple relation between the mass of the most massive cluster m_{\max} and the total mass of the molecular cloud M_{cl} ,

$$m_{\max} = 0.20M_{\text{cl}}^{0.76}. \quad (12)$$

The single line fit can be seen for the wide range $M_{\text{cl}}/M_{\odot} = 10^0 - 10^7$ (see Fig.6 in Fujii & Portegies Zwart (2015)).

We therefore combine these results, and suppose each molecular cloud forms a single BH in its core if it is more than $10M_{\odot}$, and suppose these BHs become “building blocks” of forming stellar-sized and intermediated-mass BHs. We show the number density of BHs, $n_{\text{BH}}(M_{\text{BH}})$ in Fig.5.

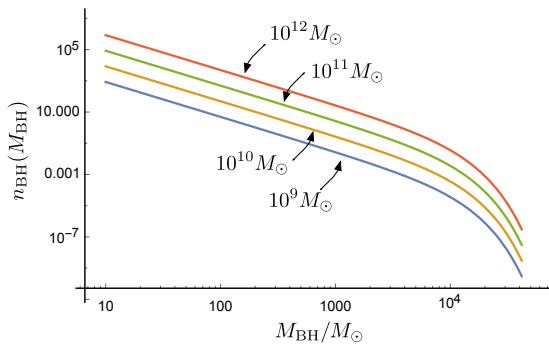


Figure 5. Number density of BHs as a function of BH mass for different total mass of galaxy $M_{\text{galaxy}} = 10^9 M_{\odot}, \dots, 10^{12} M_{\odot}$.

2.4. Numbers of BH mergers in a galaxy

In Paper I, we considered two toy models for formation of SMBHs: hierarchical growth and runaway growth. The hierarchical growth model is the case that each two nearby equal mass BHs merge simultaneously, and continue their mergers. The runaway growth model is, conversely, only one BH grows itself by continual mergers with surrounding BH companions.

The recent N-body simulations report that hierarchical merger process is plausible both for the massive clusters (10^4 - $10^6 M_{\odot}$) (see e.g. Fujii & Portegies Zwart (2015)) and for stellar-mass BHs (see e.g. Fujii *et. al.* (2016)).

We therefore simply assume that BHs formed at cores of clouds will accumulate each other hierarchically, i.e. the mass and the number of BHs at step from k to $k+1$ can be expressed simply by

$$M_{k+1} = 2M_k, \quad (13)$$

$$N_{k+1} = N_k/2. \quad (14)$$

The mass of BH merger, then, obeys the distribution

M^{-1} (see footnote ¹).

On the other hand, we know empirically the mass of the center BH of the galaxy, M_{SMBH} , and the total mass of the galaxy, M_{galaxy} , has a relation

$$M_{\text{SMBH}} = 2 \times 10^{-4} M_{\text{galaxy}} \quad (15)$$

(or equal to 10^{-3} of the bulge mass, see e.g. King (2003)).

Combining these facts, for a certain galaxy with M_{galaxy} , we pick up BHs of which total mass is M_{SMBH} (equation above), obeying its mass distribution of Fig.5. We suppose pick-upped BHs will form a SMBH in its series of mergers in hierarchical model. Together with galaxy distribution function $n_{\text{galaxy}}(M, z)$, we are able to count the possible events of BH mergers, $N_{\text{merger}}(M_{\text{BH}}, z)$, in the Universe, which we show in Fig.6.

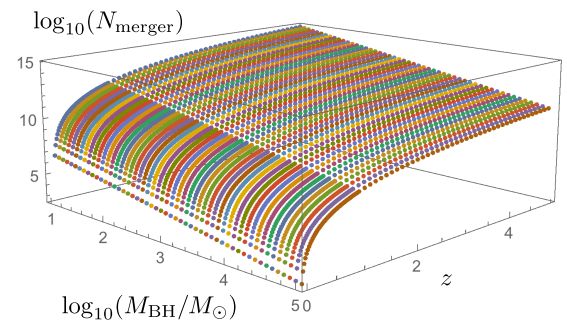


Figure 6. Cumulative distribution function (in the z direction) of BH mergers $N_{\text{merger}}(M_{\text{BH}})$. The numbers are of binned in 20 of the one order in M_{BH} .

In the next section, we further take into account the detectors’ detectable distance $D(M, a, \rho)$ (that corresponds to BH spin parameter a , energy emission rate of merger, signal-to-noise ratio ρ). In §4, we estimate the observable event rate,

$$\text{Event Rate } R[\text{yr}] = \frac{N_{\text{merger}}(z)}{V(D/2.26)}, \quad (16)$$

where the factor 2.26 is for averaging the distance for all directions (Finn & Chernoff (1993)).

3. SIGNAL-TO-NOISE RATIO (SNR)

3.1. SNR

¹ Suppose we have a cluster of the total mass M_c which consists of N_0 equal-mass BHs. This means that each BH mass is initially M_c/N_0 . They continue to form binaries and merge together, which indicates there are $N_0/2^{i-1}$ binaries for i -th generation which forms BHs with the masses $M = 2^{i-1}M_c/N_0$. The model shows only discrete distribution of the BH mass, but the number of binaries $N(M)$ can be approximated with the number of initial fractions in a cluster, $N(M) = M_c/M$.

Let the true signal $h(t)$, the function of time, is detected as a signal, $s(t)$, which also includes the unknown noise, $n(t)$:

$$s(t) = h(t) + n(t). \quad (17)$$

The standard procedure for the detection is judged by the optimal signal-to-noise ratio (SNR), ρ , which is given by

$$\rho = 2 \left[\int_0^\infty \frac{\tilde{h}(f) \tilde{h}^*(f)}{S_n(f)} df \right]^{1/2}, \quad (18)$$

where $\tilde{h}(f)$ is the Fourier-transformed quantity of the wave,

$$\tilde{h}(f) = \int_{-\infty}^\infty e^{2\pi i f t} h(t) dt, \quad (19)$$

and $S_n(f)$ the (one-sided) power spectral density of strain noise of the detector, as we showed in Fig. 1. In this paper, for KAGRA (bKAGRA), we use a fitted function

$$\sqrt{S_n(f)} = 10^{-26} \left(\frac{6.5 \times 10^{10}}{f^8} + \frac{6 \times 10^6}{f^{2.3}} + 1.5f \right), \quad (20)$$

where f is measured in Hz, as was used in Nakano *et al.* (2015).

3.2. SNR of ringdown wave

For the ringdown gravitational wave in presence of a black hole, the waveform is modeled as

$$h(t) = A \cos(2\pi f_R(t - t_0) + \psi_0) e^{-(t-t_0)/\tau} \quad (21)$$

where f_R is the oscillation frequency, and τ is the decaying time constant, t_0 and ψ_0 are the initial time and its phase, respectively (we simply set $t_0 = \psi_0 = 0$). The parameter τ is normally expressed using a quality factor, $Q \equiv \pi f_R \tau$, or $f_I = 1/(2\pi\tau)$. The waveform, (21), is then written as

$$h(t) \sim A e^{i2\pi(f_R + if_I)t} \quad (22)$$

where we call $f_R + if_I$ quasi-normal frequency, which is obtained from the perturbation analysis of black hole, and its fitting equations are shown in (3).

Following Flanagan & Hughes (1998), we use the energy spectrum formula for the ringdown wave

$$\begin{aligned} \frac{dE}{df} &= \frac{A^2 M^2 f^2}{32\pi^3 \tau^2} \\ &\times \left\{ \frac{1}{[(f - f_R)^2 + f_I^2]^2} + \frac{1}{[(f + f_R)^2 + f_I^2]^2} \right\} \\ &\approx \frac{1}{8} A^2 M^2 f_R Q \delta(f - f_R) [1 + O(1/Q)]. \end{aligned} \quad (23)$$

where M is the total mass of the binary, $M = m_1 + m_2$. We then obtain

$$E_{\text{ringdown}} \approx \frac{1}{8} A^2 M^2 f_R Q. \quad (24)$$

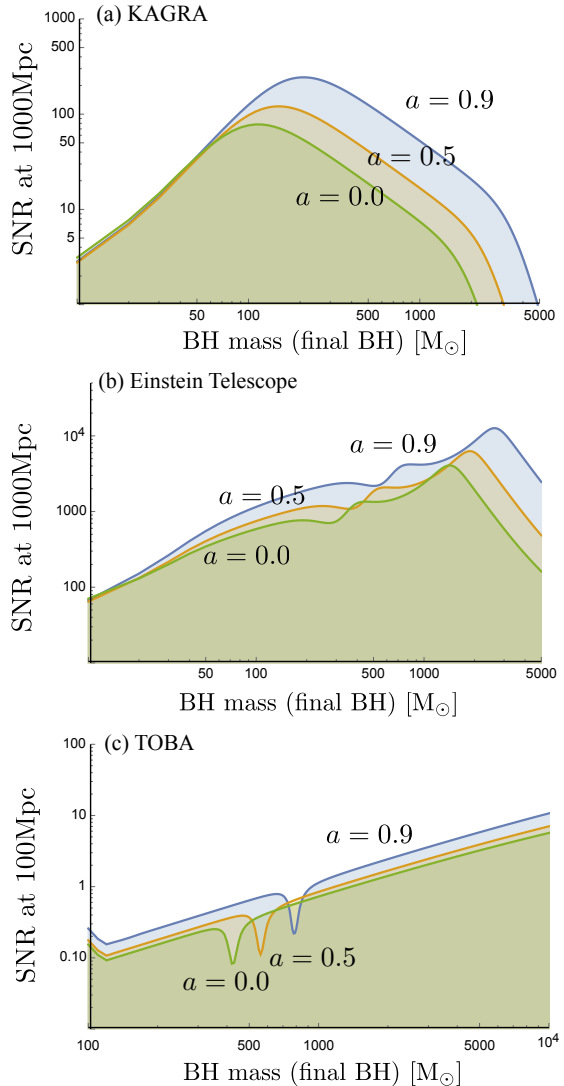


Figure 7. SNR for ring-down waves from a black hole with spin parameter a which appears at the distance 1 Gpc. Figures (a) and (b) are for KAGRA and Einstein Telescope, respectively. We see that ring-down frequencies of IMBH (especially for 100–400 M_\odot) are the best target for both KAGRA and Einstein Telescope. Figure (c) is for TOBA and the distance is estimated at 100 Mpc.

Let $\epsilon_r(a) \equiv E_{\text{ringdown}}/M$, which expresses the energy fraction of the emitted gravitation wave to the total mass. As we cited in the introduction, GW150914 and GW151226 show us $a = 0.67, 0.74$ and energy emission rate 4.6%, 4.1% of the total mass, respectively. The associated numerical simulation of GW150914

(SXS:BBH:0305)² shows that the 4.0% of the total mass is emitted before the merger³. That is, the ring-down part emits the energy around 0.6 % of the total mass. If we use $A \sim 0.4$, then we recover the ratio $\epsilon_r(0.67) = 0.58\%$ (it also produces e.g. $\epsilon_r(0.0) = 0.236\%$, $\epsilon_r(0.5) = 0.425\%$, $\epsilon_r(0.9) = 1.23\%$, $\epsilon_r(0.98) = 2.98\%$). The magnitude of this A is also consistent with the quadrupole formula.

The SNR is, then, expressed using the inertial mass $\mu = m_1 m_2 / M$ and the redshift of the source z ,

$$\rho^2 = \frac{8}{5} \frac{\epsilon_r(a)}{f_R^2} \frac{(1+z)M}{S_h(f_R/(1+z))} \times \left(\frac{(1+z)M}{d_L(z)} \right)^2 \left(\frac{4\mu}{M} \right)^2. \quad (25)$$

Up to here, we see SNR is larger when the black hole spin a is large, and has the maximum when $m_1 = m_2$.

In Fig 7, we plot SNR of ring-down waves from a BH at the distance 1 Gpc at KAGRA for $A = 0.4$. The results depends on the BH spin parameter a , but we see that ring-down frequencies of IMBH (especially for 100–400 M_\odot) are the best target for both KAGRA and Einstein Telescope.

3.3. Detectable distance

By specifying the BH mass and spin, together with ρ , then we can find the distance d_L which satisfies eq. (25). We call this distance detectable distance $D(M, a, \rho)$.

We converted Fig.7 into the plots of detectable distance D with a function of BH mass M for SNR=10 and 100. We show them in Fig.8 for KAGRA. We see the designed KAGRA covers at least 100 (10) Mpc at SNR=10 (100) for $10M_\odot < M$, and KAGRA covers 1Gpc at SNR=10 for $40M_\odot < M < 1000M_\odot$.

4. EVENT RATE

Using the detectable distance $D(M, a, \rho)$ obtained in the previous section, we set the upper limit of z for integrating eq. (10) to obtain the numbers of galaxies, N_{galaxy} , and then obtain the number of BH mergers, N_{merger} , according to the procedure shown in §2. We show N_{merger} in Fig. 9 (a1) and (b1) for SNR=10 and 30, respectively.

The event rate R , then, is estimated by eq. (16). We show them in Fig. 9 (a2) and (b2). Previous works (e.g., Miller (2002); Will (2004)) assume the number of events to the merger sources is roughly $\sim 10^{-10}$, which can be seen in our figures Fig. 9 (a1) and (a2) for higher spinning BH cases.

² SXS Gravitational Waveform Database (<https://www.black-holes.org/waveforms/>)

³ We thank Hiroyuki Nakano for pointing out this ratio.

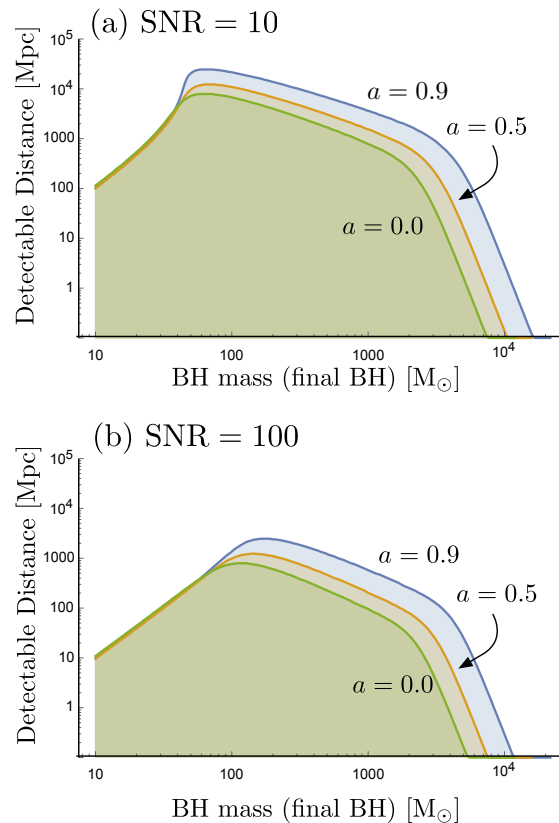


Figure 8. Detectable distance D of the ring-down signal at KAGRA. SNR is set to (a) 10 and (b) 100.

Fig. 9 is for specifying the BH spin parameter a , but if we assume that a is homogeneously distributed, then the averaged R is estimated as Fig. 10.

The event rate versus mass distribution of Fig. 10 has its peak $R \sim 7.13$ [/yr] at $M \sim 59.1M_\odot$ (200–375 [Hz] for $a = 0-0.9$). The mergers of the range $40M_\odot < M < 150M_\odot$ are $R > 1$ [/yr]. The total number of events over $R > 1$ [/yr] is ~ 211 . This property, especially the prediction of the merger over $M > 100M_\odot$ will be a key to test our model (for example, comparing with population III models by Kinugawa *et al.* (2014)).

5. SUMMARY

Based on a bottom up formation model of a super-massive black-hole (SMBH) via intermediate-mass black-holes (IMBHs), we estimate expected observational profile of gravitational wave at ground-based detectors.

At the designed KAGRA (or equivalent advanced LIGO/VIRGO), with the most standard criteria of the signal-to-noise ratio $\rho = 10$, we find the mass distribution of BH mergers has its peak at $M \sim 60M_\odot$, and we can detect also BHs at the range $40M_\odot < M < 150M_\odot$ in a certain event rates. Details numbers are, of course, depend on model parameters, but these will be clarified by accumulating actual gravitational events.

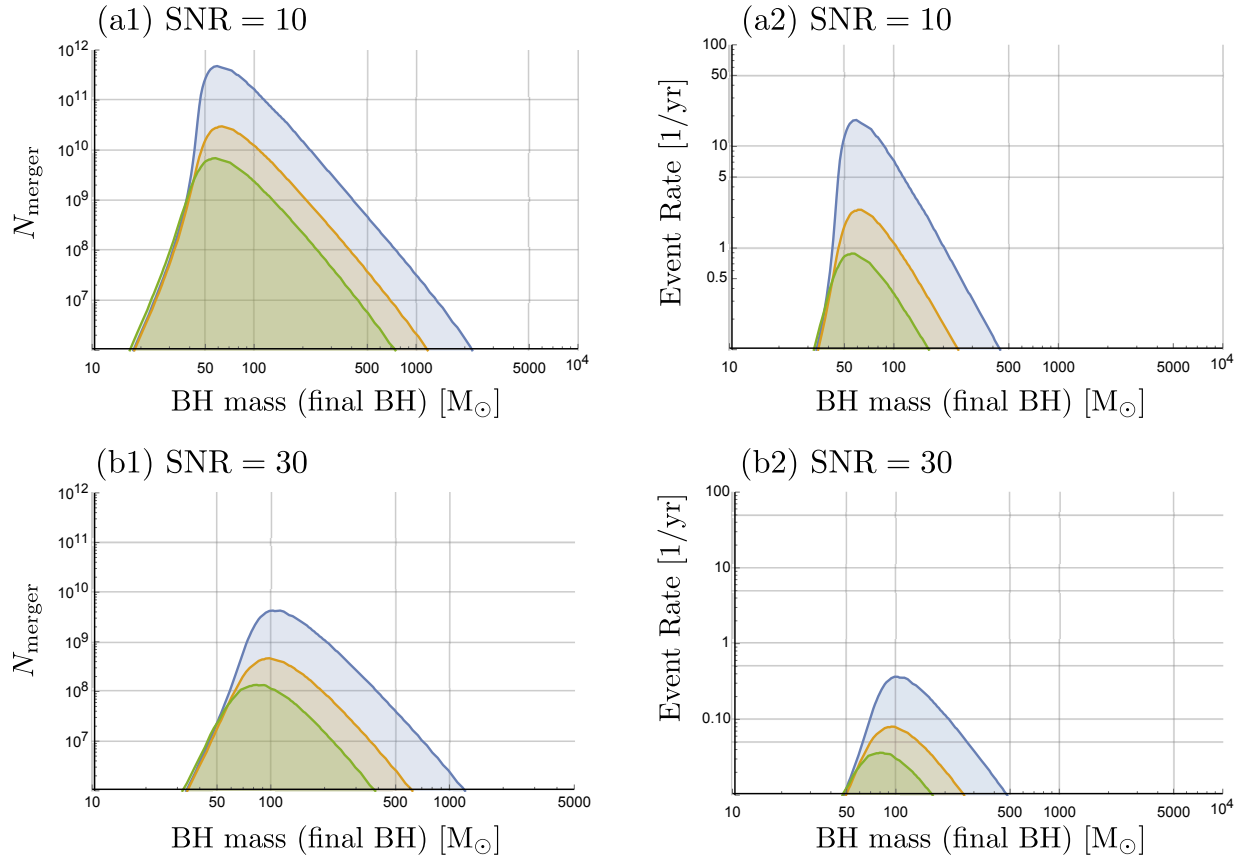


Figure 9. Event rate R as a function of BH mass M with signal-to-noise ratio $\rho = 10$ and 30 for KAGRA. Three distributions for each figure are of $a = 0.9, 0.5,$ and 0.0 (from largest to lowest), respectively.

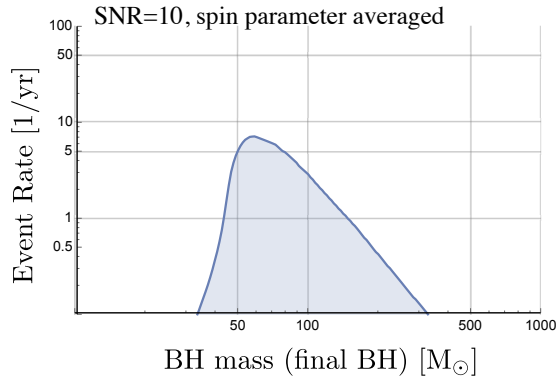


Figure 10. Event rate R as a function of BH mass M with signal-to-noise ratio $\rho = 10$ for KAGRA. Spin parameter dependences are averaged.

We conclude that the statistics of the signals will tell us both a galaxy distribution and a formation model of SMBHs, and also in future cosmological models/gravitational theories.

ACKNOWLEDGMENTS

This work was supported in part by the Grant-in-Aid for Scientific Research Fund of the JSPS (C) No. 25400277 (HS), and also by MEXT Grant-in-Aid for Scientific Research on Innovative Areas "New Developments in Astrophysics Through Multi-Messenger Observations of Gravitational Wave Sources" (No. 24103005) (NK).

REFERENCES

- Abbott, B. et al. (LIGO Scientific Collaboration and Virgo Collaboration), *PhRvL*, **116**, 061102 (2016a).
- Abbott, B. et al. (LIGO Scientific Collaboration and Virgo Collaboration), *PhRvL*, **116**, 241103 (2016b).
- Abbott, B. et al. (LIGO Scientific Collaboration and Virgo Collaboration), arXiv:1606.04856 (2016c).
- Amaro-Seoane, P., & Santamaría, L. 2010, *ApJ*, **722**, 1197.
- Ando, M., K. Ishidoshiro, K. Yamamoto, K. Yagi, W. Kokuyama, K. Tsubono, and A. Takamori, 2010, *PhRvL*, **105**, 161101.
- Belczynski, K., Taam, R.E., Kalogera, V., Rasio, F.A., Bulik, T. 2007, *ApJ*, **662** 504.
- Berti, E., Cardoso, V., & Will, C. M. 2006, *PhRvD*, **73**, 064030.
- Conselice, C.J., Wilkinson, A., Duncan, K., and Mortlock, A. 2016, *ApJ*, **830** 83.
- Ebisuzaki, T., Makino, J., Tsuru, T.G., Funato, Y, Zwart, S.P., Hut, P., McMillan, S., Matsushita, S., Matsumoto, H., & Kawabe, R. 2001, *ApJL*, **562**, L19.
- Echeverria, F. 1980, *PhRvD*, **40**, 3194.
- Finn, L. S. & Chernoff, D. F., 1993, *PhRvD***47**, 2198.
- Flanagan, É. É., and Hughes. S. A., 1998, *PhRvD*, **57**, 4535.
- Fregeau J. M. , Larson, S. L., Coleman Miller, M., O’Shaughnessy, R., & Rasio F. A. 2006, *ApJ*, **646**, L135.
- Fujii, M. S., & Portegies Zwart, S., 2015, *MNRAS*, **449**, 726
- Fujii, M. S., Tanikawa, A. & Makino, J. 2016, preprint
- Gair, J. R., Mandel, I., Coleman Miller, M., & Volonteri, M. 2011, *Gen. Rel. Grav.* **43** 485. (arXiv:0907.5450)
- Holger, B. and Makino, J., 2003, *MNRAS*, **304**, 227-246
- Inutsuka, S., Inoue, T., Iwasaki, K. & Hosokawa, T. 2015 *ã*, **580**, A49
- Ishidoshiro, K., M. Ando, A. Takamori, H. Takahashi, K. Okada, N. Matsumoto, W. Kokuyama, N. Kanda, Y. Aso, and K. Tsubono, 2011, *PhRvL*, **106**, 161101.
- Iwasawa, M., An, S., Matsubayashi, T., Funato, Y., & Makino, J., 2010, arXiv:1011.4017
- King, A. 2003, *ApJL*, **596**, L27.
- Kinugawa, T., Inayoshi, K., Hotokezaka, K., Nakauchi, D. & Nakamura, T. 2014, *MNRAS*, **442**, 2963.
- Kinugawa, T., Miyamoto, A., Kanda, N. & Nakamura, T. 2016, *MNRAS*, **456**, 1093.
- Leaver, E. W. 1985, *Proc. R. Soc. Lond.* **A402**, 285.
- Marchant, A. B., Shapiro, S. L., 1980, *ApJ*, **239**, 685.
- Matsubayashi, T., Makino, J., & Ebisuzaki, T. 2007, *ApJ*, **656**, 879.
- Matsubayashi, T., Shinkai, H., & Ebisuzaki, T., 2004, *ApJ*, **614**, 864. (Paper I)
- Matsumoto *et. al.* 2001, *ApJL*, **547**, L25.
- Matsushita *et. al.* 2000, *ApJL*, **545**, L107
- Miller, M. C. 2002, *ApJ*, **581**, 438
- Nakano, H., Tanaka, T., & Nakamura, T. 2015, *PhRvD*, **92**, 064003
- Portegies Zwart, S. F., Makino, J., McMillan, S. L. W., and Hut, P., 1999, *A&A*, **348**, 117
- Portegies Zwart, S. F., and McMillan, S. L. W., 2002, *ApJ*, **528**, L17
- Portegies Zwart, S. F., and McMillan, S. L. W., 2002, *ApJ*, **576**, 899
- Portegies Zwart, S. F., Holger, B., Piet, H., Makino, J., and McMillan, S. L. W., 2004, *Nature*, **428**, 724
- Rees, M. J. 1978, *Observatory* **98**, 210; Rees, M. J. 1984, *Annu. Rev. Astron. Astrophys.* **22**, 471.
- Robertson, B.E., Ellis, R.S., Dunlop, J.S., McLure, R.J., & Stark, D.P. 2010, *Nature*, **468** 55.
- Robertson, B.E. & Ellis, R.S. 2012, *ApJ*, **744** 95.
- Sheth, R.K., & Tormen, G., 1999, *MNRAS*, **308**, 119
- Sudou, H., Iguchi, S., Murata. Y., and Taniguchi Y., 2003, *Science*, **300**, 1263
- Vale, A., & Ostriker, J.P., 2006, *MNRAS*, **371**, 1173
- Will, C. M. 2004, *ApJ*, **611**, 1080